Exp Fluids (2015) 56:83
DOI 10.1007/s00348-015-1950-6

RESEARCH ARTICLE

A low-cost, precise piezoelectric droplet-on-demand generator

Daniel M. Harris[1] · Tanya Liu[2] · John W. M. Bush[1]

Received: 17 February 2015 / Revised: 17 March 2015 / Accepted: 21 March 2015 / Published online: 10 April 2015

Abstract We present the design of a piezoelectric droplet-on-demand generator capable of producing droplets of highly repeatable size ranging from 0.5 to 1.4 mm in diameter. The generator is low cost and simple to fabricate. We demonstrate the manner in which droplet diameter can be controlled through variation of the piezoelectric driving waveform parameters, outlet pressure, and nozzle diameter.

1 Introduction

Under certain conditions, bouncing droplets on a vibrating fluid bath can achieve lateral propulsion across the fluid surface through interaction with their own wave field (Protiere et al. 2006; Moláček and Bush 2013). These walking droplets exhibit many features reminiscent of microscopic quantum particles (Couder and Fort 2006; Eddi et al. 2009; Fort et al. 2010; Harris et al. 2013; Bush 2015) and so are the subject of considerable interest. In early experiments, droplets were created by rapidly extracting a partially submerged pin from a fluid bath by hand (Protiere et al. 2006). It is now known that the dynamical behavior of these droplets is strongly dependent on their size (Moláček and Bush 2013; Wind-Willassen et al. 2013). Consequently, repeatable experiments require a reliable and precise droplet generation technique.

Repeatable droplet generation is also required for a number of diverse applications ranging from inkjet printing to liquid crystal display manufacturing (Fan et al. 2008). A variety of droplet-on-demand (DOD) generators are described in the literature, but most existing designs are complex, costly, and difficult to adopt for use in other studies. Many systems are designed for the generation of droplets smaller than 500 μm in diameter (Bransky et al. 2009; Reis et al. 2005; Meacham et al. 2005; Perçin and Khuri-Yakub 2003; Cheng and Chandra 2003; Goghari and Chandra 2008; Chen and Basaran 2002; Dong et al. 2006; Switzer 1991), below the desired range for the walking droplet experiments. We here describe a simple, repeatable DOD system designed specifically for this range, 0.5–1.3 mm (Protiere et al. 2006; Moláček and Bush 2013).

The present device is inspired by the design of Yang et al. (1997) which ejects a droplet from a nozzle at the base of a fluid chamber by contracting a piezoelectric disk sealed to the top of the chamber. They used a fixed fluid reservoir and custom-fabricated glass nozzles. For a range of nozzles 125–250 μm in diameter, they found an overall variability in size of <10 % of the measured droplet diameters (<500 μm). Their device has since been adopted for relatively large-scale drop (diameters >500 μm) generation (Mehdizadeh et al. 2004; Hawke 2006).

Castrejón-Pita et al. (2008) used a loudspeaker to actuate their DOD generator and fabricated interchangeable nozzle plates ranging from 0.15 to 3.00 mm in diameter. A fluid reservoir of adjustable height allowed for control of the pressure at the nozzle outlet. For fixed control parameters, the device was stated to have an overall variability of droplet size of <5 %. Terwagne (2011) successfully designed and employed a DOD generator to produce droplets for their own bouncing

Electronic supplementary material The online version of this article (doi:10.1007/s00348-015-1950-6) contains supplementary material, which is available to authorized users.

✉ John W. M. Bush
bush@math.mit.edu

[1] Department of Mathematics, Massachusetts Institute of Technology, Cambridge, MA 02139, USA

[2] Department of Mechanical Engineering, Massachusetts Institute of Technology, Cambridge, MA 02139, USA

droplet experiments (Terwagne et al. 2013). Using a piezoelectric disk for actuation, an air pump for pressure regulation, and an excimer-laser machined orifice for droplet ejection, they produced droplets with diameters ranging from 100 μm to a few millimeters with a variation in diameter of ±3 %.

We here describe a droplet generator design that aims to surpass existing systems in terms of affordability, simplicity, and precision. The generator is capable of producing highly repeatable droplets with diameters in the range of 0.5–1.4 mm with <1 % variability. All components of the design can be purchased for less than a few hundred dollars and fabricated using only manual mill and lathe equipment. A fluid reservoir of variable height is used for pressure regulation, and the only electrical components necessary are a DC power supply, Arduino board, and H-bridge circuit. The generator is tested with 20 cS silicone oil over a range of operating parameters, and the effects of these parameters on droplet diameter are examined.

2 Droplet generator description

The droplet generator consists of five main components: piezoelectric disk, fluid chamber, nozzle, adjustable-height fluid reservoir, and fluid pump (Fig. 1). The piezoelectric actuator is a commercially available piezoelectric buzzer (CUI CEB-35D26, diameter 35 mm, available at Digi-Key: 102-1128-ND). To create an airtight seal between the piezoelectric and fluid chamber orifice, the piezoelectric is first bonded to the top of the fluid chamber with an RTV silicone sealant and then secured in place by an acrylic ring that provides a clamping force on the edges of the piezoelectric. The brass base of the piezoelectric disk is in direct contact with the working fluid; consequently, a pressure pulse is generated in the fluid chamber by the voltage-induced flexure of the disk.

The fluid chamber is a cylinder of 28.6 mm diameter and depth 9.7 mm bored out of an aluminum block. The cylindrical chamber tapers down to a tapped hole in the bottom of the chamber where the nozzle is attached and sealed to the base of the generator with an O-ring. Eight stainless steel nozzles ranging from 0.50 to 1.40 mm in outlet diameter with a 45° outer taper were machined and tested. The outer taper discouraged the fluid from wetting the outer surface of the nozzle.

The fluid pressure at the nozzle plane must be regulated so that a stable fluid meniscus forms at the nozzle outlet; specifically, the contact line of the fluid coincides with the lip of the nozzle outlet (Fig. 1, inset). If the fluid pressure is too high, fluid will drip or flow out of the nozzle continuously, and if it is too low, air will be drawn into the chamber.

A height-adjustable fluid reservoir is connected to the fluid chamber. The reservoir consists of two concentric cylinders 69.9 and 50.8 mm in diameter mounted onto a micrometer drive translation stage (Thor Labs PT1). A small peristaltic pump (Williamson 100 series) pumps fluid into the inner cylinder which overflows into the outer cylinder, thereby maintaining a constant fluid level in the inner cylinder. The height of the reservoir relative to the nozzle outlet determines the hydrostatic pressure at the outlet. Static equilibrium requires that this hydrostatic pressure be balanced by the capillary pressure at the outlet, determined by the adaptive shape of the meniscus (Fig. 1, inset). A range of reservoir heights, $|\Delta h| \leq 2\sigma/\rho g a$, may thus support a static equilibrium, where σ and ρ are the surface tension and density of the fluid, respectively, g is the acceleration due to gravity, and a is the radius of the nozzle outlet.

All air bubbles must be eliminated from the fluid chamber; otherwise, the applied pressure pulse may lead to gas compression rather than liquid ejection. To accomplish this, the generator is inverted and held at a lower height until fluid bleeds from the nozzle. The nozzle tip is then sealed with an elastic band while the chamber is restored to the upright position. The elastic band is then removed, and

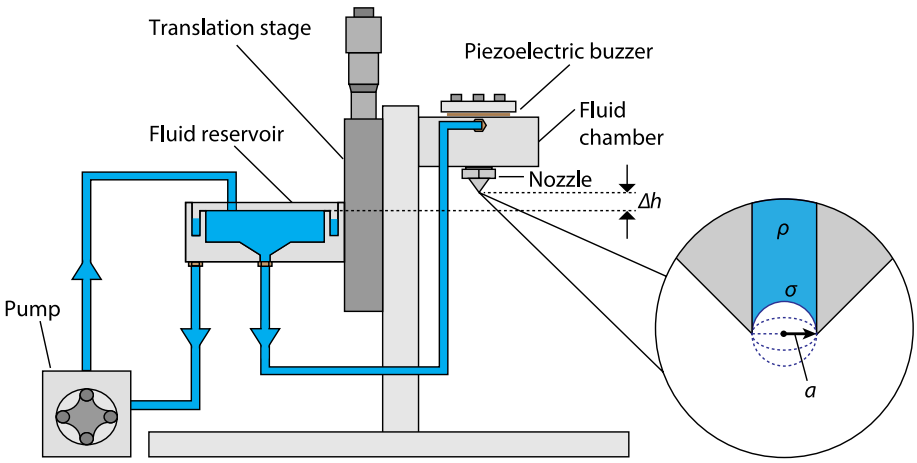

Fig. 1 Schematic of droplet generator. *Inset* the form of the static meniscus at the nozzle outlet depends on Δh, the difference between the reservoir and nozzle heights. As Δh increases, the fluid recedes into the nozzle. Stable static menisci arise for $|\Delta h| \leq 2\sigma/\rho g a$. The schematic is not drawn to scale. Technical drawings for all components are available in the supplementary materials

the exterior of the nozzle dried with a lint-free cloth, again to discourage wetting of its outer surface. During normal operation, this bleeding procedure need only be performed once at the beginning of the experiments.

The electrical components used for driving the piezoelectric element consist of an adjustable DC power supply (0–72 V), H-bridge circuit, and Arduino Uno microcontroller. The piezoelectric piece is driven by a square voltage waveform, an example of which is shown in Fig. 2. When not in use, the piezoelectric piece is supplied with a constant negative voltage. The sudden application of a positive voltage causes the piezoelectric piece to contract and generates a positive pressure pulse in the chamber that forces liquid through the nozzle. Reverting to a negative voltage causes the piezoelectric to expand and creates a negative pressure fluctuation that draws liquid back into the chamber. Under the right operating conditions, this sequence of expansion and contraction expels a single droplet from the nozzle. While studies have been done on the effect of driving waveform shape on droplet generation (Chen and Basaran 2002; Dong et al. 2006), we employ a square waveform in order to simplify the required circuitry.

Arduinos are microcontroller boards commonly used for rapid prototyping projects. Two digital output pins of the Arduino Uno are connected to an H-bridge circuit, which allows for the rapid reversal of the polarity of the applied voltage to the piezoelectric element. The two electrical control parameters are thus the amplitude (voltage) and the duration (pulse width) of the square pulse. The pulse width of the piezoelectric driving waveform can be controlled to high precision, with a resolution of 1 μs. To ensure precise timing, interrupts were disabled during critical portions of the Arduino timing code. This simple electrical system eliminates the need for a pulse generator (or function generator and amplifier) as is typically used in such devices (Yang et al. 1997; Terwagne 2011; Castrejón-Pita et al. 2008).

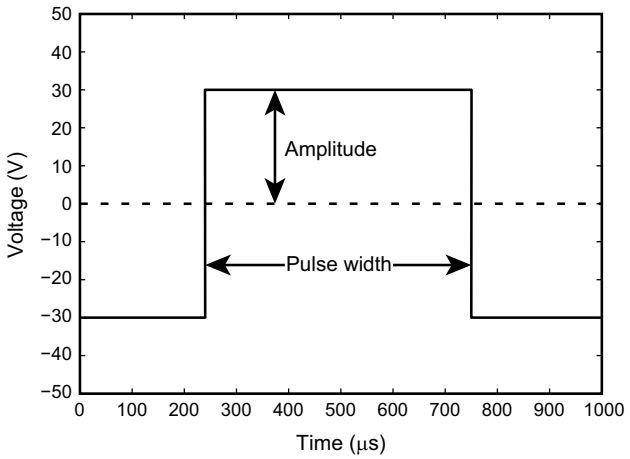

Fig. 2 Example of a typical waveform used to drive the piezoelectric element

3 Experimental setup

In order to assess the repeatability of the system, the droplet generator is placed between a 20-W LED light source and a high-speed camera (Phantom v5.2, macro lens, 2× teleconverter, tube extension). A single image is captured per droplet generated. The timing of the image capture is synchronized with the droplet generator by a trigger signal sent to the camera by the Arduino. In a typical image capture sequence, the Arduino triggers a voltage pulse sent to the piezoelectric piece, waits for a specified delay time (typically between 15 and 80 ms), and then triggers the camera system to capture an image.

After image collection, droplet diameter data are extracted from the images with a Canny edge detection algorithm in MATLAB (Canny 1986). The algorithm finds edges in an image by identifying local discontinuities in intensity and then fits an ellipse to the detected droplet edge using a least-squares method. The equivalent diameter of the droplet in pixels is then calculated from the volume of the axially symmetric ellipsoid inferred from the fitted ellipse (Fig. 3). The diameter measurement in pixels is converted to millimeters using the mm/pixel resolution calculated using a microscope calibration slide and is found to be 3.27 ± 0.02 μm/pixel. Henceforth, error bars reported for diameter measurements represent the combination of uncertainty from this calibration resolution and actual variation in droplet diameters. When the error bar is not visible, its extent is exceeded by the marker size.

All experiments reported below were conducted with the fluid used in the walking droplet experiments, 100 % pure silicone oil of density $\rho = 950$ kg/m^3, surface tension $\sigma = 0.0206$ N/m, and kinematic viscosity $\nu = 20.9 \pm 0.1$ cSt. We can assess the relative influence of viscous and capillary forces by the Ohnesorge number: $Oh = \frac{\mu}{\sqrt{\sigma R_n \rho}}$ where $\mu = \rho\nu$ is the dynamic viscosity of the fluid and R_n is the radius of the nozzle. For the present experiments, $0.16 < Oh < 0.28$, indicating that viscosity has a relatively minor dynamical influence. We thus expect the trends reported here to hold for fluids of comparable or lower viscosities. At least 2500 images are captured and analyzed for each diameter measurement presented in the following sections. Droplets are generated at a frequency of 5 Hz. Below approximately 10 Hz, the droplet size was independent of the driving frequency. The generator can thus be operated at arbitrarily slow generation rates (in true DOD mode) without change of behavior or performance.

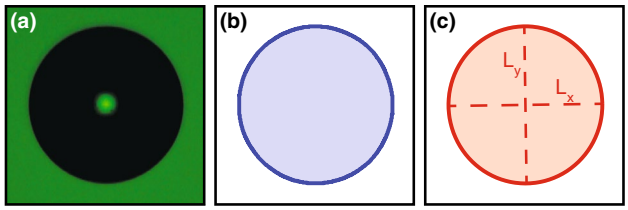

Fig. 3 **a** Typical droplet photo prior to image processing for diameter inference. **b** Fitted ellipse from edge detection. **c** Principal axes of ellipse used to calculate the volume of the ellipsoid assuming axial symmetry about the vertical axis. The equivalent droplet diameter is calculated from this ellipsoid volume

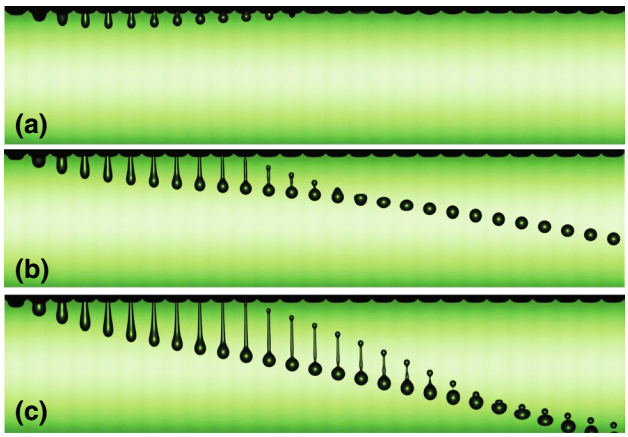

Fig. 4 Dependence of droplet generation on pulse width for the same nozzle diameter (1.40 mm) and applied voltage (30 V). **a** No droplet is generated with a 460-μs pulse width. **b** A single droplet is generated with a 660-μs pulse width. **c** Multiple droplets are generated with a 850-μs pulse width. Neighboring images are separated by 1 ms

4 Results

For a given nozzle, a range of parameters exist for which a single droplet is ejected. Previous studies have shown that the size and behavior of ejected droplets depend on the pulse width and voltage of the piezoelectric driving waveform (Fan et al. 2008; Reis et al. 2005; Shin et al. 2011; Tsai and Hwang 2008). Figure 4 shows the changing system behavior as the pulse width is increased. In Fig. 4a, the pulse width is too short for droplet generation to occur. With an increased pulse width (Fig. 4b), a single droplet is successfully generated. When the pulse width is increased further, a secondary droplet pinches off from the tail of the primary droplet (Fig. 4c). In general, a range of pulse widths exists for which a single droplet is formed.

Figure 5a shows that when other control parameters are fixed, the ejected droplet diameter tends to increase with increasing pulse width. For a pulse width of 380 μs, the measured droplet diameter achieves its minimum: No droplet generation occurs below this limit. Above the upper pulse width limit of 540 μs, satellite droplet formation occurs. Between these limits, a single droplet is generated. If the pulse width is held fixed, the voltage can be used as the primary control parameter (Fig. 5b). Upper and lower voltage limits then exist, above which satellite droplets form and below which no droplets are generated, respectively.

To explore the influence of the nozzle outlet pressure, drop diameter measurements were taken over a range of equilibrium fluid reservoir heights, for which there was no dripping or air intake. We denote by Δh the difference between the reservoir height and nozzle plane: $\Delta h = 0$ when the reservoir surface is aligned with the nozzle outlet

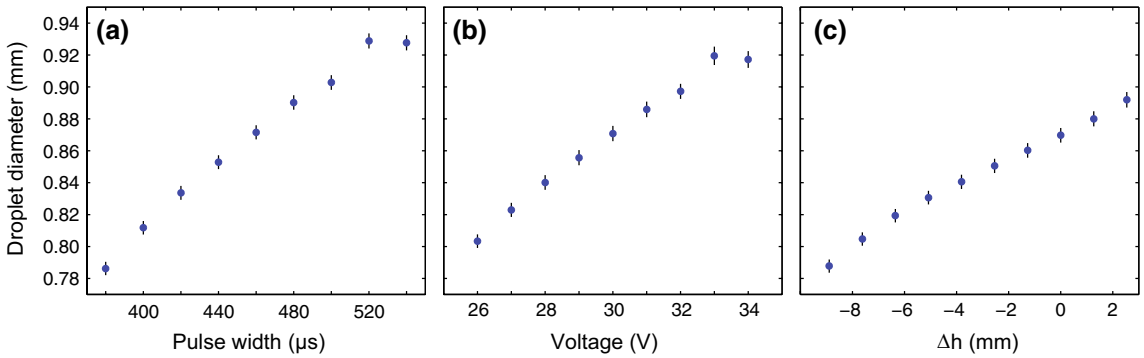

Fig. 5 Influence of electrical control parameters on droplet diameter with a 0.90-mm diameter nozzle. **a** Effect of pulse width variation with amplitude 30 V and reservoir height $\Delta h = 0$. **b** Effect of voltage amplitude with 460 μs pulse width and $\Delta h = 0$. **c** Effect of reservoir height with pulse amplitude of 30 V and pulse width of 460 μs

(Fig. 1). Figure 5c shows the dependence of droplet diameter on Δh for a fixed voltage and pulse width.

To compare the operation of the generator with and without the pump, 5000 droplets were generated while the pump was running, and 5000 more with the pump turned off. A comparison of the droplet diameters in Fig. 6 indicates a steady decrease in droplet diameter without the use of the pump. This dependence is consistent with that on reservoir height. The decrease in measured diameter is <2 % after 5000 droplets. The pump is thus unnecessary for applications requiring only a small number of droplets. Increasing the diameter of the fluid reservoir would also minimize this effect.

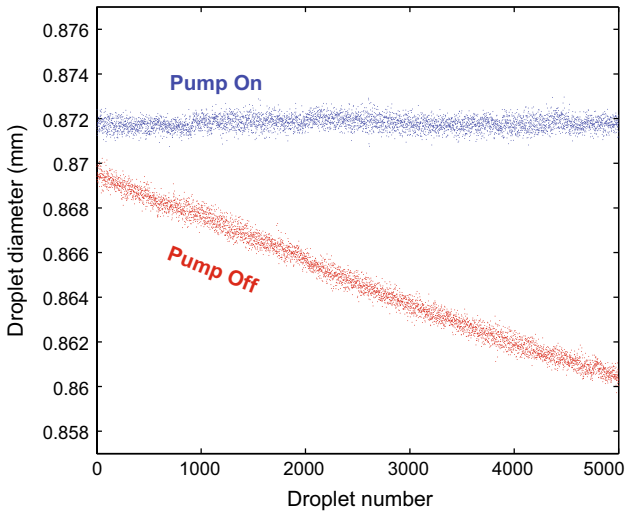

Fig. 6 Comparison of droplet generation with and without the peristaltic pump that replenishes the reservoir. Without the pump, the droplet diameter steadily decreases as the fluid in the reservoir is depleted. Data are obtained for the 0.90-mm diameter nozzle, voltage of 30 V, and pulse width of 460 μs

Eight different nozzles ranging from 0.50 to 1.40 mm in diameter were fabricated and tested with the droplet generator. The upper and lower pulse width limits at a fixed voltage were measured for each nozzle and are reported in Fig. 7a. Droplet diameter measurements taken at these limits, reported in Fig. 7b, represent the largest and smallest achievable droplets for a given nozzle. While the droplet diameter is roughly determined by the nozzle diameter (Chen and Basaran 2002), variation of the pulse width allows for a range of droplet sizes to be produced with a given nozzle.

Our results indicate that the generation process is highly repeatable for a single run. Diameter measurements of over 2500 droplets generated with the same operating parameters have variations of <0.5 %. Another relevant diagnostic for laboratory used is the day-to-day repeatability, the system's robustness to disturbance. To assess this diagnostic, an air bubble was intentionally introduced into the fluid chamber and removed using the bleeding procedure. This process was repeated multiple times with diameter data taken after each trial, and the results are shown in Fig. 8. Even with such disturbances, the variation in droplet diameter across multiple trials is still within ±1 %. This additional uncertainty may be caused by slight differences in the pinning of the contact line at the nozzle outlet after the exterior of the nozzle is dried, or minor variations in the image calibration (mm/pixel) between runs.

5 Conclusion and recommendations

We have presented and evaluated the potential of a simple piezoelectric droplet generator designed for use in experimental studies of walking droplets. The droplet size is

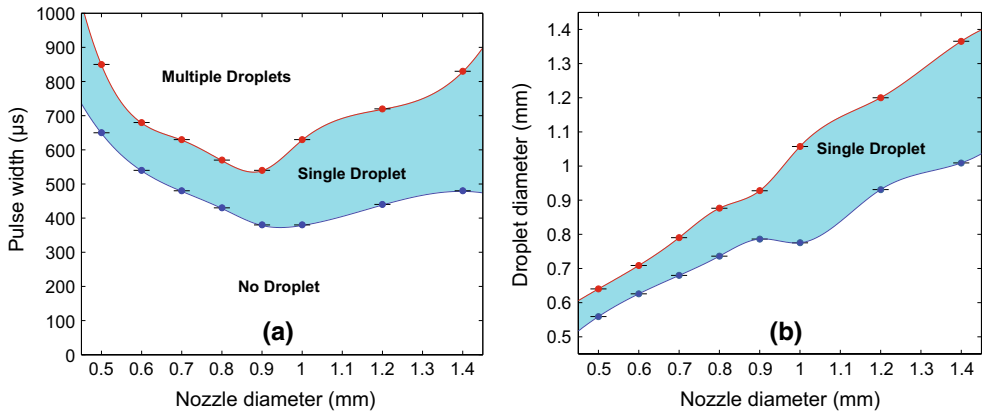

Fig. 7 **a** *Upper* and *lower curves* represent the upper and lower pulse width limits for single droplet generation from nozzles with different diameters with a fixed voltage (30 V) and reservoir height ($\Delta h = 0$). **b** Droplet diameters for each nozzle evaluated at upper and lower pulse width limits

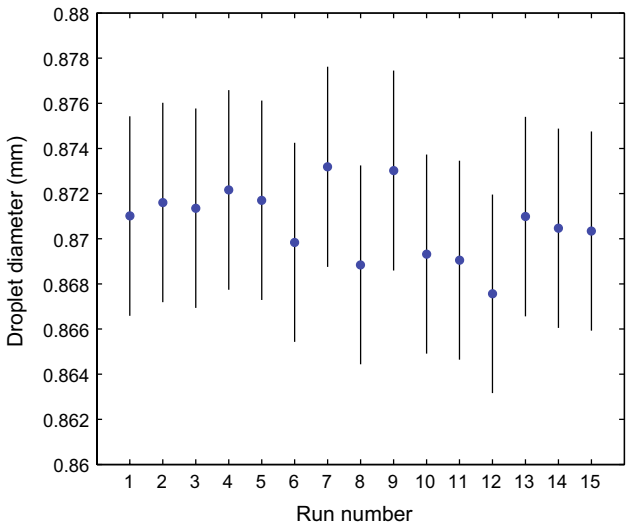

Fig. 8 Day-to-day repeatability of droplet diameters generated from a 0.90-mm diameter nozzle with a pulse width of 460 μs and voltage of 30 V. Between each measurement, air was introduced into the chamber and the bleeding procedure repeated

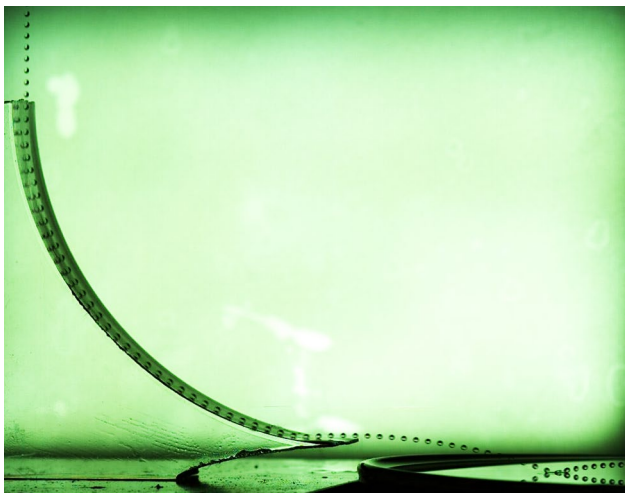

Fig. 9 To deposit the droplets onto the fluid bath, they are directed down a curved surface wetted with a thin layer of silicone oil

roughly prescribed by the nozzle diameter; nevertheless, a range of droplet sizes can be generated through variation of either the pulse width, voltage, or reservoir height. For a single run, droplet diameters are repeatable to within ± 0.5 %, while the day-to-day variation in droplet diameter is approximately ±1 %. This droplet generator is simpler than its predecessors, but still achieves satisfactorily repeatable results. The generator is low cost and simple to manufacture. All necessary components of the present design can be purchased for less than a few hundred dollars. A redesign of the generator for fabrication via rapid prototyping

Fig. 10 A stable lattice of oil droplets formed with our droplet generator bounces on the surface of a vibrated oil bath

techniques such as 3D printing could further lower the manufacturing cost.

The high repeatability and range of droplet diameters producible from this generator design make it an excellent candidate for use in walking droplet experiments. To avoid coalescence in depositing the droplets onto the vibrating bath, we direct the droplets down a curved surface prewetted by a thin layer of silicone oil applied with a brush (Gilet and Bush 2012) as shown in Fig. 9. The drops thus impact the bath surface at an acute angle, thereby skipping and rolling before settling into a stable bouncing or walking state. Multiple bouncing droplets created in this fashion can self-organize into stable lattice arrangements (Eddi et al. 2009) as demonstrated in Fig. 10.

Acknowledgments The authors gratefully acknowledge the financial support of the NSF through Grants CBET-0966452 and CMMI-1333242; D. M. H. was supported through the Graduate Research Fellowship Program. The authors thank L. Tambasco for help with the initial experiments.

References

Bransky A, Korin N, Khoury M, Levenberg S (2009) A microfluidic droplet generator based on a piezoelectric actuator. Lab Chip 9(4):516–520

Bush JWM (2015) Pilot-wave hydrodynamics. Annu Rev Fluid Mech 47(1):269–292

Canny J (1986) A computational approach to edge detection. IEEE Trans Pattern Anal Mach Intell 6:679–698

Castrejón-Pita JR, Martin GD, Hoath SD, Hutchings IM (2008) A simple large-scale droplet generator for studies of inkjet printing. Rev Sci Instrum 79(7):075108

Chen AU, Basaran OA (2002) A new method for significantly reducing drop radius without reducing nozzle radius in drop-on-demand drop production. Phys Fluids 14:L1–L4

Cheng S, Chandra S (2003) A pneumatic droplet-on-demand generator. Exp Fluids 34(6):755–762

Couder Y, Fort E (2006) Single particle diffraction and interference at a macroscopic scale. Phys Rev Lett 97(154):154101

Dong H, Carr WW, Morris JF (2006) An experimental study of drop-on-demand drop formation. Phys Fluids 18(7):072102

Eddi A, Fort E, Moisy F, Couder Y (2009) Unpredictable tunneling of a classical wave-particle association. Phys Rev Lett 102(24):240401

Eddi A, Decelle A, Fort E, Couder Y (2009) Archimedean lattices in the bound states of wave interacting particles. Europhys Lett 87:56002

Fan KC, Chen JY, Wang CH, Pan WC (2008) Development of a drop-on-demand droplet generator for one-drop-fill technology. Sens Actuators A Phys 147(2):649–655

Fort E, Eddi A, Boudaoud A, Moukhtar J, Couder Y (2010) Path-memory induced quantization of classical orbits. Proc Natl Acad Sci 107(41):17515–17520

Gilet T, Bush JWM (2012) Droplets bouncing on a wet, inclined surface. Phy Fluids 24(12):122103

Goghari AA, Chandra S (2008) Producing droplets smaller than the nozzle diameter by using a pneumatic drop-on-demand droplet generator. Exp Fluids 44(1):105–114

Harris DM, Moukhtar J, Fort E, Couder Y, Bush JWM (2013) Wave-like statistics from pilot-wave dynamics in a circular corral. Phys Rev E 88(1):011001

Hawke SR (2006) Effects of a thin, flexible nozzle on droplet formation and impingement. Ph.D. thesis, Oregon State University

Meacham JM, Varady MJ, Degertekin FL, Fedorov AG (2005) Droplet formation and ejection from a micromachined ultrasonic droplet generator: visualization and scaling. Phys Fluids 17(10):100605

Mehdizadeh NZ, Chandra S, Mostaghimi J (2004) Formation of fingers around the edges of a drop hitting a metal plate with high velocity. J Fluid Mech 510:353–373

Moláček J, Bush JWM (2013) Drops walking on a vibrating bath: towards a hydrodynamic pilot-wave theory. J Fluid Mech 727:612–647

Perçin G, Khuri-Yakub BT (2003) Piezoelectric droplet ejector for ink-jet printing of fluids and solid particles. Rev Sci Instrum 74(2):1120–1127

Protiere S, Boudaoud A, Couder Y (2006) Particle–wave association on a fluid interface. J Fluid Mech 554:85–108

Reis N, Ainsley C, Derby B (2005) Ink-jet delivery of particle suspensions by piezoelectric droplet ejectors. J Appl Phys 97(9):094903

Shin P, Lee S, Sung J, Kim JH (2011) Operability diagram of drop formation and its response to temperature variation in a piezoelectric inkjet nozzle. Microelectron Reliab 51(2):437–444

Switzer GL (1991) A versatile system for stable generation of uniform droplets. Rev Sci Instrum 62(11):2765–2771

Terwagne D (2011) Bouncing droplets, the role of deformations. Ph.D. thesis, Université de Liège

Terwagne D, Ludewig F, Vandewalle N, Dorbolo S (2013) The role of the droplet deformations in the bouncing droplet dynamics. Phys Fluids 25(12):122101

Tsai MH, Hwang WS et al (2008) Effects of pulse voltage on the droplet formation of alcohol and ethylene glycol in a piezoelectric inkjet printing process with bipolar pulse. Mater Trans 49(2):331–338

Wind-Willassen Ø, Moláček J, Harris DM, Bush JWM (2013) Exotic states of bouncing and walking droplets. Phys Fluids 25(082):082002

Yang JC, Chien W, King M, Grosshandler WL (1997) A simple piezoelectric droplet generator. Exp Fluids 23(5):445–447